iodosyl chloride so formed is likely to be in an electronically or vibrationally excited state.

Mechanism of Iodyl Chloride Formation. Since irradiation of matrices containing scrambled $^{16}O_{3-x}{}^{18}O_x$ or $^{16}O_3$ and $^{18}O_3$ in the ratio 1:1 both yielded O_2ICl with a random distribution of oxygen isotopes, the two oxygen atoms in O_2ICl originate in different O_3·ICl complex molecules. The relative yield of O_2ICl and OICl increases in favor of the dioxo species as the photolysis temperature is increased which, together with the isotope data, implies that the formation of O_2ICl is diffusion controlled. It is proposed that electronically or vibrationally excited OICl formed during photolysis of O_3·ICl is either quenched, forming the observed iodosyl chloride product, or decomposes releasing an oxygen atom for reaction with another OICl to give O_2ICl.

Conclusions

Codeposition of ozone and iodine monochloride in argon, krypton, and nitrogen matrices leads to the formation of a specific molecular complex, O_3·ICl. The complex photodissociates to iodosyl chloride OICl with visible light. The OICl photoproduct is probably formed initially in a vibrationally or electronically excited state and is either quenched by the matrix or dissociates to ICl and atomic oxygen. The release and diffusion of oxygen atoms leads to formation of a second product iodyl chloride O_2ICl. Iodyl chloride becomes the favored product as the photolysis temperature is increased as a result of either a greater extent of diffusion of oxygen atoms through the matrix or a reduced efficiency in the quenching of excited iodosyl chloride.

This paper represents the first characterization of a monomolecular inorganic iodosyl compound. Normal coordinate analysis calculations applied to iodyl chloride treated the IO_2 moiety as vibrationally independent of the chlorine atom: frequencies for $\nu_{sym}(IO_2)$, $\nu_{asym}(IO_2)$, and $\delta(IO_2)$ for three isotopes $^{16}O_2ICl$, $^{18}O_2ICl$, and $^{16}O^{18}OICl$ could be fitted within experimental error. This implies little mechanical or electronic influence of the chlorine atom on the vibrations of the IO_2 moiety as a result of the large mass of iodine and substantial ionic character in the I–Cl bond. Polarity in the I–Cl bond is supported by the low frequency of the I–Cl stretching mode compared with iodine monochloride and the high frequency of the symmetric and antisymmetric stretching vibrations of the IO_2 group.

Acknowledgement is made to the donors of the Petroleum Research Fund, administered by the American Chemical Society, for support of this research and to the Science Research Council (U.K.) for a research studentship (D.J.D.).

Study of Disaccharide Conformation by Measurements of Nuclear Overhauser Enhancement, Relaxation Rates, and ^{13}C–^{1}H Coupling: 1,6-Anhydro-β-cellobiose Hexaacetate

Photis Dais,* Tony K. M. Shing, and Arthur S. Perlin

Contribution from the Department of Chemistry, McGill University, Montreal, Quebec H3C 3G1, Canada. *Received June 9, 1983*

Abstract: Nonselective and mono- and biselective spin–lattice relaxation rates, nuclear Overhauser enhancements, and coupling constants were measured as means for determining such stereochemical features as the conformation of the glucosidic bond of 2,3,4,6,2′,3′-hexa-*O*-acetyl-4-*O*-β-D-glucopyranosyl-1′,6′-anhydro-β-D-glucopyranose (**1**) in acetone-d_6 solution. Interproton distances within each ring of **1**, as well as of **2**, specifically C-deuterated samples of **1**, calculated from either a combination of monoselective relaxation rates and NOE experiments or mono- and biselective relaxation rates, agreed within ±0.2 Å of those found in the crystal. However, substantially different values were obtained from nonselective relaxation rate measurements. The orientation of the glucosidic bond, as deduced from interresidue spin–spin coupling (^3J) between the C-1,H-4′ and C-4′,H-1 nuclei, is described by dihedral angles ψ of 45–50° and ϕ of 25–30°. These values are within the region of the allowed conformation as defined by the interatomic distances H-1–H-4′ and H-1–H-5′ obtained from relaxation, NOE data, and by computer simulation.

The conformational properties of disaccharides have received a great deal of attention in recent decades, stimulated primarily by interest in the conformations of structurally related polysaccharides. There are various theoretical treatments of the subject,[1,2] and several experimental techniques have been employed to determine disaccharide conformations in the solid state[3-5] and in solution.[6-10]

One approach for examining conformation in solution is offered by proton monoselective spin–lattice relaxation experiments in combination with NOE data,[11,12] and/or mono- and biselective experiments[13] that determine the magnitude of specific dipolar interproton spin–lattice relaxation contributions. This approach has been utilized in the present study for the quantitative measurement of interproton distances within disaccharide derivative **1**, i.e., 2,3,4,6,2′,3′-hexa-*O*-acetyl-4-*O*-β-D-glucopyranosyl-1′,6′-anhydro-β-D-glucopyranose (1,6-anhydro-β-cellobiose), in order to determine its conformation in solution. Compound **1** attracted

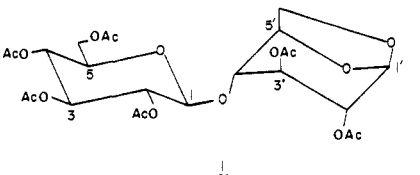

1

our interest because it introduces a marked departure in stereochemistry from other derivatives of cellobiose examined previously.[9,10] Among other differences, the reducing end moiety of **1** possesses the opposite ($^1C_4$) chair conformation, and its (1→4′) linkage entails an axial, rather than equatorial, *O*-4′. In earlier

(1) Rees, D. A.; Skerrett, R. J. *Carbohydr. Res.* **1968**, *7*, 334.
(2) Rees, D. A.; Smith, P. J. C. *J. Chem. Soc., Perkin Trans.* **1975**, *2*, 836.
(3) Quigley, G. J.; Sarko, A.; Marchessault, R. H. *J. Am. Chem. Soc.* **1970**, *92*, 5834.
(4) Ham, J. T.; Williams, D. G. *Acta Crystallogr., Sect. B* **1970**, *26*, 1373.
(5) Chu, S. S. C.; Jeffrey, G. A. *Acta Crystallogr., Sect. B* **1968**, *24*, 830.
(6) Casu, B.; Reggiani, M.; Gallo, G. G.; Vigevani, A. *Tetrahedron* **1966**, *22*, 3061.
(7) Rees, D. A. *J. Chem. Soc., B* **1970**, 877.
(8) Perlin, A. S.; Cyr, N.; Ritchie, R. G. S.; Parfondry, A. *Carbohydr. Res.* **1974**, *37*, C1.
(9) Parfondry, A.; Cyr, N.; Perlin, A. S. *Carbohydr. Res.* **1977**, *59*, 299.
(10) Hamer, G. K.; Balza, F.; Cyr, N.; Perlin, A. S. *Can. J. Chem.* **1978**, *56*, 3109.
(11) Hall, L. D.; Wong, K. F. *J. Chem. Soc., Chem. Commun.* **1979**, 951.
(12) Hall, L. D.; Hill, H. D. W. *J. Am. Chem. Soc.* **1976**, *98*, 1269.
(13) Kaplan, D.; Navon, G. *J. Chem. Soc., Perkin Trans. 2* **1981**, 1374.

0002-7863/84/1506-3082$01.50/0

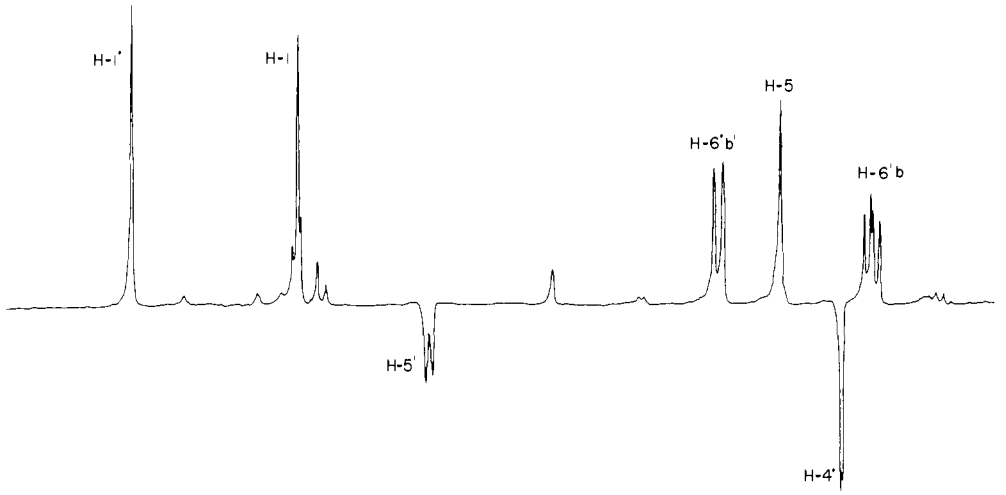

Figure 1. Representative ^1H spin–lattice relaxation experiment with **2**, at 400 MHz. The H-4′ and H-5′ resonances were inverted simultaneously by two consecutive, selective, 180° pulses (~50 ms each) provided by the decoupler channel.

investigations,[8-10] which included α-D-glucosides, the orientations of glycosidic bonds were assessed from interresidue $^{13}C-^1H$ coupling. Measurements of the latter parameter in **1** also are described here, and their relative merits and limitations are considered in the light of the relaxation data obtained. Overall, the structural problem was greatly alleviated by the preparation of **2**, a specifically deuterated analogue of **1**.

Experimental Section

The ^1H NMR experiments were conducted at 400 and 200 MHz, and ^{13}C NMR experiments at 100 MHz, with a Bruker WH-400 and a Varian XL-200 spectrometer, respectively. A probe temperature of 20 °C was used for ^1H relaxation measurements, and of 21 °C for those of ^{13}C. The solutions of **1** were 0.05 M in acetone-d_6 for all relaxation and NOE experiments. Each sample was carefully degassed by performing five to six "freeze–pump–thaw" cycles, and the tube was then sealed. ^{13}C spin–lattice relaxation times and ^1H nonselective relaxation rates were measured by the (180°–t–90°–T) inversion recovery sequence. Details of the procedure used in the nonselective relaxation and NOE experiments are given elsewhere.[14]

Monoselective relaxation rates of individual protons in partially deuterated **1** were measured by using a long (30–40 ms), weak preirradiation pulse at the required resonance frequency.[15] The selective 180° pulse was provided by the decoupler channel. In performing the bi- (double) selective experiments, the computer of the spectrometer was used to control a train of two selective 180° pulses provided consecutively by the decoupler at two resonance frequencies chosen. Although the time interval between these two pulses was negligible (~200 ns), the duration of the consecutive selective pulses is an important practical limitation to the selectivity of the frequency with which an individual experiment could be performed. That is, the occurrence of significant relaxation during excitation would limit the effectiveness of the experiment. This was particularly important for the methylene protons, which are characterized by fast relaxation rates. Nevertheless, the biselective relaxation rates of most of the proton pairs (as will be shown in Table III) relative to the duration of the selective pulses (total duration of two pulses, ~100 ms), ensured the effectiveness of these experiments. A typical biselective inversion of a pair of protons is shown in Figure 1. Mono- and biselective partially relaxed spectra were obtained by the inversion recovery method. Each relaxation rate value presented is an average of two to three separate measurements, and the statistical error and reproducibility of the various NMR parameters are shown as footnotes in the tables.

Analysis of ^1H-Coupled ^{13}C spectra. Spectra were analyzed by computer simulation using the ITRCL program,[16] with a Nicolet B-NC 12 model computer interfaced to a Bruker WH-90 spectrometer. A first-order AMRX analysis was made for C-1 of deuterated **1**, whereas second-order analyses (ABMQRX) were carried out for the C-4′ and C-5′ signals of deuterated **1** and the C-3′ signal of **1**. The required ^1H and ^{13}C NMR parameters (J and $\Delta\nu$) were obtained from the corresponding spectra recorded at 400 MHz and, in each case, the analysis involved a systematic variation of the line width to obtain the best visual fit between simulated and observed spectra. It is estimated that the error in the values of ^2J and ^3J is ±0.03–0.05 Hz.

Preparation of 2′,3′,2,3,4,6-Hexa-*O*-acetyl-d_{18}-4-*O*-β-D-glucopyranosyl-1,6-anhydro-β-D-glucopyranose-2′,3′,2,3,4,6a,6a′-d_7 (2). The procedure was analogous to that used for the deuteration of methyl β-cellobioside.[10] A solution of 4-*O*-β-D-glucopyranosyl-1,6-anhydro-β-D-glucopyranose (1.4 g) in deuterium oxide (40 mL), containing Raney nickel catalyst (7 g, preexchanged with deuterium oxide), was heated under reflux for 24 h. The mixture was filtered through Celite, the filtrate was concentrated, and the greenish, syrupy, residue was acetylated with acetic anhydride (5 mL) and pyridine (5 mL). When a solution of the product in ethanol (7 mL) was seeded with the title compound (nondeuterated specimen), 0.39 g of crystals was recovered, following which the material remaining was subjected to chromatography on Celite, affording an additional 0.54 g of the required product. The combined crops of crystals (mp 143–144 °C) was de-O-acetylated with sodium methoxide in methanol (0.47 M) for 4 h, Amberlite IR-120 (H^+) resin was introduced, the suspension was filtered, and the filtrate was acetylated with acetic-d_6 anhydride (2 mL) and pyridine (2 mL). Workup furnished the title compound (**2**, 0.55 g) as colorless needles, mp 142–143 °C. The ^{13}C NMR spectrum of the product (see also its partial ^1H NMR spectrum in Figure 1) indicated that carbons 2, 3, 4, 6, 2′, and 3′ were deuterated to the extent of ≥90%.

Geometry of 1. No experimental data giving specific details about the structure of **1** could be found in the literature. Consequently, values of interproton distances in the 2,3,4,6-tetra-*O*-acetyl-β-D-glucopyranosyl and 2′,3′-di-*O*-acetyl-1′,6′-anhydro-β-D-glucopyranose moieties were derived from crystallographic data for β-cellobiose octaacetate,[17a] β-cellobiose,[17b] 2,3,4-tri-*O*-acetyl-1,6-anhydro-β-D-glucopyranose,[18a] and 1,6-anhydro-β-D-glucopyranose.[18b] These values are to be found in Table V.

The orientation of the glucosidic linkage as a function of the interatomic distances between the H-1,H-4′ and H-1,H-5′ protons as the ϕ and ψ angles are varied is expressed in the form of a "conformational map", which determines the combinations of angles permitted by the NMR criteria. In other words, it shows the allowed conformations of **1** compatible with interatomic distances H-1–H-4′ and H-1–H-5′ (within ±0.2 Å), as calculated from the NMR data. These interproton distances were generated by a program written in such a way that each pair of H-1–H-4′ and H-1–H-5′ distances was sufficient to classify a given conformation. The angles were sampled at intervals of 10°, in the usual way,[19] without restrictions imposed by contact between adjacent residues, i.e., $\phi = -180$ to 180° and $\psi = 0$ to 360°. Conformation $\phi = \psi = 0$ was defined[19] as having H-4′ and H-1 in the same plane as C-1–O-4′–C-4′, and the apex of the C-1–O-4′–C-4′ angle pointing in the same sense as the C-4′–H-4′ bond and in the sense opposite to the C-1–H-1 bond. To convert a model of **1** in this form, into any conformation (ϕ, ψ), the anhydroglucopyranose

(14) Dais, P.; Perlin, A. S. *Can. J. Chem.* **1982**, *60*, 1648.
(15) Freeman, R.; Hill, J. D. W.; Tomlinson, B. L.; Hall, L. D. *J. Chem. Phys.* **1974**, *61*, 4466.
(16) ITRCL Nicolet Instrument Corp., Madison, WI., 1974.
(17) (a) Leung, F.; Chanzy, H. D.; Perez, S.; Marchessault, R. H. *Can. J. Chem.* **1976**, *54*, 1365. (b) Chu, S. S. C.; Jeffrey, G. A. *Acta Crystallogr., Sect. B* **1968**, *24*, 830.
(18) (a) Leung, F.; Marchessault, R. H. *Can. J. Chem.* **1974**, *52*, 2516. (b) Park, Y. J.; Kim, H. S.; Jeffrey, G. A. *Acta Crystallogr., Sect. B* **1971**, *27*, 220.
(19) Rees, D. A.; Scott, W. E. *J. Chem. Soc. B* **1971**, 469, and references therein.

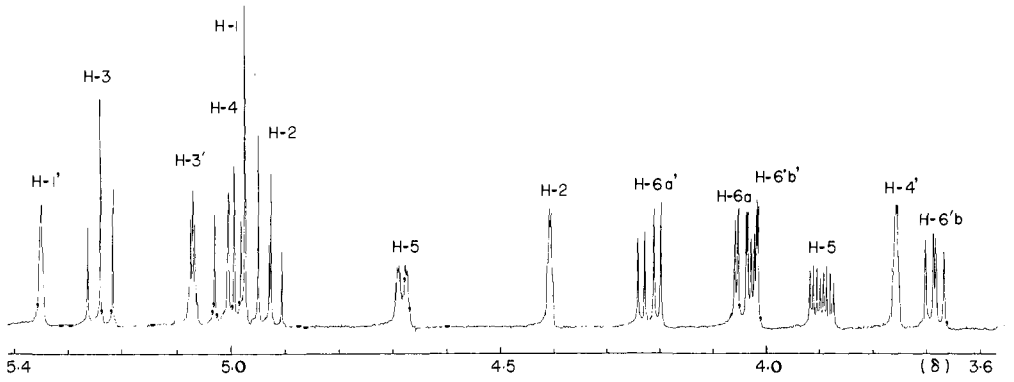

Figure 2. ^{1}H NMR spectrum of **1** (0.05 M in acetone-d_6) at 400 MHz (temp 20 °C).

Table I. ^{1}H and ^{13}C Chemical Shifts (δ) and Coupling Constants (Hz) for 2,3,4,6,2',3'-Hexa-*O*-acetyl-4-*O*-β-D-glucopyranosyl-1,6-anhydro-β-D-glucopyranose (1)

proton	δ^1H	$J_{H,H}$		carbon	δ^{13}C	$^1J_{C,H}$		$^2J_{C,H}$		$^3J_{C,H}$	
H-1	4.99	$^2J_{H-6a,H-6a'}$	12.21	C-1	100.64	$J_{C-1,H-1}$	162.90	$J_{C-3',H-2'}$	−4.29	$J_{C-1,H-5}$	3.49
H-2	4.94	$^2J_{H-6',H-6'b'}$	7.75	C-2[b]	71.78	$J_{C-2,H-2}$	144.28	$J_{C-3',H-4'}$	−4.29	$J_{C-1,H-4'}$	3.30
H-3	5.25	$^3J_{H-1,H-2}$	8.14	C-3	73.78	$J_{C-3,H-3}$	146.13	$J_{C-4',H-5'}$	−4.80	$J_{C-2',H-3}$	5.04
H-4	5.02	$^3J_{H-2,H-3}$	9.50	C-4[b]	69.12	$J_{C-4,H-4}$	151.08	$J_{C-5',H-4'}$	−3.24	$J_{C-1',H-5'}$	6.09
H-5	3.90	$^3J_{H-3,H-4}$	9.50	C-5	72.51	$J_{C-5,H-5}$	153.24	$J_{C-5',H-6'b}$	−1.00	$J_{C-1',H-6'b'}$	3.29
H-6a	4.05	$^3J_{H-4,H-5}$	10.09	C-6	62.57	$J_{C-6,H-6a}$	147.38			$J_{C-3'H-1'}$	4.43
H-6a'	4.22	$^2J_{H-5,H-6a}$	5.25			$J_{C-6,H-6a'}$	147.95			$J_{C-3',H-5'}$	4.43
H-1'	5.36	$^3J_{H-5,H-6a'}$	2.44	C-1'	99.72	$J_{C-1',H-1'}$	176.73			$J_{C-4',H-1}$	4.20
H-2'	4.42	$^3J_{H-1',H-2'}$	1.40	C-2'[c]	69.92	$J_{C-2',H-2'}$	152.74			$J_{C-4',H-6'b'}$	4.20
H-3'	5.08	$^3J_{H-2',H-3'}$	3.10	C-3'[c]	70.19	$J_{C-3',H-3'}$	158.92			$J_{C-5',H-1'}$	5.18
H-4'	3.77	$^3J_{H-3',H-4'}$	3.10	C-4'	77.20	$J_{C-4',H-4'}$	148.32			$J_{C-6'H-1'}$	5.39
H-5'	4.69	$^3J_{H-4',H-5'}$	1.60	C-5'	74.39	$J_{C-5'H-5'}$	159.21			$J_{C-4'H-6'b}$	8.15
H-6'b	3.69	$^3J_{H-5',H-6'b}$	5.95	C-6'	65.51	$J_{C-6',H-6'b}$	153.42				
H-6'b'	4.04	$^3J_{H-5',H-6'b'}$	1.10			$J_{C-6',H-6'b'}$	153.42				
	2.03	$^4J_{H-1',H-3'}$	1.40		19.91						
	2.01	$^4J_{H-2',H-4'}$	1.10	CH_3	19.77						
CH_3	1.97	$^4J_{H-3',H-5'}$	1.25		19.62						
	1.95				19.55						
	1.94										
	1.90				170.14						
					169.70						
				C=O	169.64						
					169.34						
					169.30						
					169.05						

[a] Notations a and b refer to the geminal protons of the glucopyranosyl and 1,6-anhydroglucopyranose residues, respectively. [b,c] Assignments may be interchanged. [d] Negative values for ^2J assumed, according to ref 24.

ring is held stationary and viewed from the glucopyranosyl end, while the glucopyranosyl residue is rotated anticlockwise, through ψ, about C-4'–O-4', and clockwise, through ϕ, about the O-4'–C-1 bond. Values of 116.8° were taken for the C-1–O-4'–C-4' angle and values of 1.43, 1.43, and 1.52 Å for the C-1–O-4', C-4'–O-4', and C-4'–C-5' bonds, respectively.

Results and Discussion

At 400 MHz, the ^{1}H NMR spectrum of **1** was fully resolved and first order (Figure 2), whereas its spectrum at 200 MHz showed second-order features and overlapping resonances. The assignments listed for the proton resonances in Table I were straightforward, especially with the aid of homodecoupling and reference to ^{1}H NMR data[20-22] for monosaccharide derivatives corresponding to the two residues of **1**. Also given in Table I are the ^{13}C chemical shifts, which were determined by selective decoupling with both **1** and **2**, and reference to literature data for 1,6-anhydrohexopyranoses.[23] Uncertainty remains in the assignments of the C-2,C-4 and C-2' and C-3' signals, although the corresponding $^1J_{C-H}$ couplings (Table I) may be helpful in this context. No attempt was made to assign the individual signals produced by the protons or carbon nuclei of the *O*-acetyl groups.

^{1}H and ^{13}C Coupling Data. Many features of the geometry of **1** are evident in the spin–spin coupling data summarized in Table I. The interpretation of coupling between the various vicinal protons of the 2,3,4,5-*O*-tetraacetyl-β-D-glucopyranosyl moiety of disaccharide **1** is consistent with the $^4C_1$ conformation adopted by the β-D-glucopyranosyl ring, namely, $^3J_{H-1,H-2}$ = 8.14 Hz, $^3J_{H-2,H-3}$ = 9.50 Hz, $^3J_{H-3,H-4}$ = 9.50 Hz, and $^3J_{H-4,H-5}$ = 10.09 Hz. Similarly, the spectrum of the 1,6-anhydro-β-D-glucopyranose segment of **1** exhibits ^{1}H–^{1}H couplings across four bonds (^4J), since the protons involved have the "planar W" relationship.[20-22,25]

The H-6'b and H-6'b' methylene protons,[26] comprising the AB portion of a three-spin ABX system in which X represents H-5', exhibit a minor splitting ($^3J_{H-5',H-6'b'}$ = 1.10 Hz) and a major splitting ($^3J_{H-5',H-6'b}$ = 5.95 Hz). These values indicate that the projected bond angles between H-5'–H-6'b' and H-5'–H-6'b are approximately 90 and 30°, respectively, as in 1,6-anhydro-β-D-glucopyranose triacetate.[20,24] Signal H-5' appears as a doublet of narrow quartets, the major splitting of which is due to coupling with H-6'b, whereas the further separation into a total of eight lines indicates splittings with H-6'b', H-4', and H-3'. The coupling $^3J_{H-4',H-5'}$ = 1.60 Hz was verified with the deuterated compound

(20) Heyns, K.; Weyer, J. *Justus Liebeg Ann. Chem.* **1968**, *718*, 224.
(21) Hall, L. D.; Manville, J. F.; Tracey, A. *Carbohydr. Res.* **1967**, *4*, 514.
(22) Cerny, M.; Stanek, J., Jr. *Adv. Carbohydr. Chem. Biochem.* **1977**, *34*, 24.
(23) Ritchie, R. G. S.; Cyr, N.; Perlin, A. S. *Can. J. Chem.* **1976**, *54*, 2301.
(24) Schwarcz, J. A.; Cyr, N.; Perlin, A. S. *Can. J. Chem.* **1975**, *53*, 1872. Cyr, N.; Hamer, G. K.; Perlin, A. S. *Ibid.* **1978**, *56*, 297.
(25) Sternhell, S. *Rev. Pure Appl. Chem.* **1964**, *14*, 15.
(26) The notations H-6'b and H-6'b' are used for the exo and endo methylene protons of the 1,6-anhydroglucopyranose ring, respectively, whereas H-6a and H-6a' are the methylene protons of the glucopyranosyl ring.

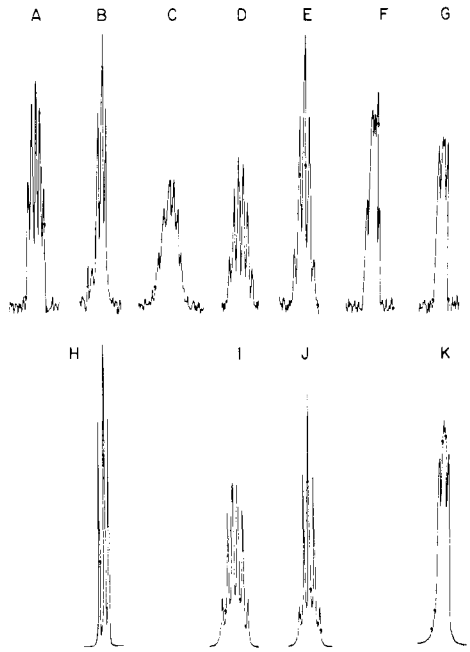

Figure 3. One-half of the 100-MHz ^{1}H-coupled ^{13}C NMR spectra of (A) C-1 of **1**, (B) C-1 of **2**, (C) C-4′ of **1**, (D) C-4′ of **2**, (E), C-3′ of **1**, (F) C-5′ of **1**, and (G) C-5′ of **2**. Spectra H, I, J, and K are simulations corresponding to B, D, E, and G, respectively.

(**2**), in which H-2′ and H-3′ were replaced by deuterium, because its spectrum exhibited an H-4′ doublet of J = 1.60 Hz, which must be due to coupling with H-5′. Similarly, the splitting $^4J_{H\text{-}3',H\text{-}5'}$ = 1.25 Hz observed in the spectrum of **1** was absent from the spectrum of **2**. Although H-5′ also might be expected to show coupling with H-1′, none was detected, nor has it been observed with the monomeric derivative.[21,22,25] The well-resolved H-3′ quintet consists of equal couplings with H-2′ and H-4′ ($^3J_{H\text{-}2',H\text{-}3'} \simeq {}^3J_{H\text{-}3',H\text{-}4'} \simeq$ 3.10 Hz) and, additionally, with H-1′ and H-5′ ($^4J_{H\text{-}1',H\text{-}3'}$ = 1.4 Hz, $^4J_{H\text{-}3',H\text{-}5'}$ = 1.25 Hz). Signal H-2′ is a narrow doublet of triplets, due to its splitting by H-3′, and weaker coupling with H-1′ and H-4′ ($^3J_{H\text{-}1',H\text{-}2'}$ = 1.4 Hz, $^4J_{H\text{-}2',H\text{-}4'}$ = 1.1 Hz), whereas the H-4′ signal is a quintet reflecting a major splitting (3.1 Hz) by H-3′, and additional splittings by H-2′ and H-5′. The H-1′ triplet exhibits equal coupling with H-2′ and H-3′, which is clearly apparent in the spectrum of **2** in which the H-1′ resonance has collapsed to a sharp singlet, due to the deuteration at positions 2′ and 3′.

Far greater complexity is found in the ^{1}H-coupled ^{13}C spectrum of **1**. Of principal concern here are the C-1 resonances of the glucopyranosyl group and that of C-4′ of the 1,6-anhydroglucose residue, because they characterize the orientation of the glucosidic linkage. Carbon-1 produces a doublet of almost equally spaced quintets (Figure 3A), due to coupling with H-1 (^1J = 162.90 Hz), and also with H-5, H-2, and H-4′. Irradiation at the resonance frequency of H-3 had no effect on the signal, thus confirming that $^3J_{C\text{-}1,H\text{-}3}$ = 0. Decoupling of H-2, either by selective irradiation or deuteration (as in **2**), converts the C-1 signal into a doublet of triplets, as shown in Figure 3B. Although no coupling is observed between C-1 and H-5′, the latter couples with H-4′ ($^3J_{H\text{-}4',H\text{-}5'}$ = 1.60 Hz) and $\Delta\nu_{4',5'}$ is large (Table I). By treating C-1 as the X part of an AMRX spin system in which J_{MX} ($J_{C\text{-}1,H\text{-}5'}$ = 0) gives the triplet shown in Figure 3H, which closely reproduces the experimentally observed signal ($^1J_{C\text{-}1,H\text{-}1}$ = 162.90 Hz, $^3J_{C\text{-}1,H\text{-}5}$ = 3.49 Hz, and $^3J_{C\text{-}1,H\text{-}4'}$ = 3.30 Hz) (Figure 3B and Table I).

The C-4′ signal of the 1,6-anhydrohexose moiety (Figure 3C) is a doublet ($^1J_{C\text{-}4',H\text{-}4'}$ = 148.32 Hz) of multiplets reflecting two-bond coupling with H-3′ and/or H-5′, and three-bond coupling with H-1, H-2′, and the 6,6′ protons. In the spectrum of **2**, the multiplets are resolved into well-defined sextets (Figure 3D), with spacings of ~4 Hz each, because there no longer are splittings due to H-2′ and H-3′. The analysis of this sextet structure was facilitated by selective ^{1}H-decoupling. Thus, on sequential irradiation of H-1, H-5′, and H-6′b′, signal 3D was reduced in each instance to a quintet of ~4.5 Hz spacings. Moreover, when H-6′b was selectively irradiated, its coupling with C-4′ was found to be ~8 Hz, as shown by the quartet produced.

A simulation of the C-4′ signal of **2**, consistent with these observations, was carried out by treating the C-4′ nucleus as part of a six-spin system including H-1, H-4′, H-5′, H-6′b, and H-6′b′. With the use of appropriate chemical shifts, and coupling parameters of $^3J_{C\text{-}4',H\text{-}1}$ = 4.2 Hz, $^2J_{C\text{-}4',H\text{-}5'}$ = −4.8 Hz, $^3J_{C\text{-}4',H\text{-}6'b'}$ = 4.2 Hz, and $^3J_{C\text{-}4',H\text{-}6'b}$ = 8.1 Hz (Table I), the simulated signal (Figure 3I) closely reproduced the experimental one (Figure 3D).

For comparison with the (doublet of) quintets produced by C-3′ (Figure 3E), the use of parameters $^3J_{C\text{-}3',H\text{-}1'} = {}^3J_{C\text{-}3',H\text{-}5'}$ = 4.43 Hz, and $^2J_{C\text{-}3',H\text{-}2'} = {}^2J_{C\text{-}3',H\text{-}4'}$ = −4.29 Hz (Table I) afforded the simulated C-3′ quintet shown in Figure 3J. The poorly resolved splitting pattern that characterizes C-5′ (Figure 3F) is appreciably clarified when position 3′ is deuterated, as seen from the corresponding signal in the spectrum of **2** (Figure 3G). Computer simulation (Figure 3K), confirming the closely spaced quintet structure of the C-5′ signal of **2**, afforded the following parameters: $^3J_{C\text{-}5',H\text{-}1'}$ = 5.18 Hz, $^2J_{C\text{-}5',H\text{-}4'}$ = −3.24 Hz, $^2J_{C\text{-}5',H\text{-}6'b}$ = −1.0 Hz, and $^2J_{C\text{-}5',H\text{-}6'b'}$ = 0 (Table I).

Among other signals examined by first-order analysis were those of C-2 of **1** and C-1′, C-6′ of **2**. The C-2 signal appears as a doublet of doublets, in which $^1J_{C\text{-}2,H\text{-}2}$ = 144.28 Hz, whereas the smaller splitting of 5.04 Hz is due to coupling with H-3; this was confirmed through substitution of H-3 by deuterium, which caused the C-2 signal to collapse to a doublet. The C-6′ signal of **2**, also a doublet of doublets that is partially overlapped, has a large spacing of 153.42 Hz and a small one of 5.39 Hz. Irradiation of H-1′ removed the latter splitting, confirming that $^3J_{C\text{-}6',H\text{-}1'}$ = 5.39 Hz, leaving two doublets of equal coupling ($^1J_{C\text{-}6',H\text{-}6'b} = {}^1J_{C\text{-}6',H\text{-}6'b'}$ = 153.42 Hz). Although the C-1′ signal in deuterated **2** was a clearly visible doublet of quartets, the corresponding signal in **1** appeared as a doublet of broad multiplets. Irradiation of H-6′b removed the smaller splitting, i.e., $^3J_{C\text{-}1',H\text{-}6'b}$ = 3.29 Hz, whereas irradiation of H-5′ removed the larger coupling, $^3J_{C\text{-}1',H\text{-}5'}$ = 6.09 Hz.

Conformation of 1 from Coupling Data. The magnitude of the long-range couplings $^4J_{H\text{-}2',H\text{-}4'}$ = 1.1 Hz and $^4J_{H\text{-}3',H\text{-}5'}$ = 1.25 Hz, together with the fact that $^3J_{H\text{-}2',H\text{-}3'} = {}^3J_{H\text{-}3',H\text{-}4'}$ = 3.10 Hz, is consistent with a $^1C_4$ conformation for the 1,6-anhydroglucopyranose ring, in accord with earlier findings.[18,20-22,25] Similarly, the vicinal couplings (4.43 Hz) of C-3′ with H-1′ and H-5′ are commensurate with a large dihedral angle relating C-3′ with those two protons, as required for the $^1C_4$ conformation. Contributing[27,28] to the absence of observed coupling between C-6′ and H-4′ is their gauche relationship, as well as the trans orientation of the pendant O-4′ and O-6′ atoms with respect to the coupling pathway. It is noteworthy that when C-6 and H-4 are anti, as in 1,6-anhydro-β-D-galactopyranose,[29] the coupling is large (5.2 Hz).

Rotamer populations of the glucosidic bond should be reflected in coupling constants $^3J_{C\text{-}4',H\text{-}1}$ and $^3J_{C\text{-}1,H\text{-}4'}$, as their magnitude is determined by the orientation of the two monosaccharide residues relative to the C-1–H-4′ and C-4′–H-1 bonds,[8-10] which are described by torsional angles ϕ and ψ in projection formulas **3** and **4**. On the basis of the measured couplings, and an appropriate Karplus curve,[10] ϕ and ψ are estimated to be about 25–30 and 45–50°, respectively. The value of ψ differs somewhat from that of methyl β-cellobioside heptaacetate,[10] although it is very

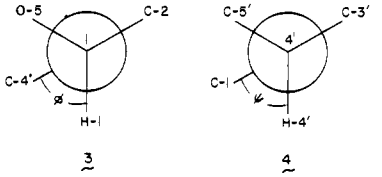

3 **4**

(27) Schwarcz, J. A.; Perlin, A. S. *Can. J. Chem.* **1972**, *50*, 3667.
(28) Hansen, P. E. *Progr. NMR Spectrosc.* **1981**, *14*, 175.
(29) Bock, K.; Pederson, C. *Acta Chem. Scand., Sect. B* **1977**, *31*, 354.

Table II. ^{13}C Spin–Lattice Relaxation Times of the Ring Carbons of 1[a]

carbon	T_1 (s)[b]	carbon	T_1 (s)[b]
C-1	1.00	C-1'	0.99
C-2	1.00	C-2'	1.00
C-3	1.01	C-3'	1.01
C-4	1.03	C-4'	1.02
C-5	0.99	C-5'	0.99
C-6	0.63	C-6'	0.52

[a] 0.05 M in acetone-d_6 at 21 °C. [b] Statistical error of the two parameter fit ~ ±5%, and reproducibility better than ±10%.

close to the dihedral angle in β-maltose peracetate, as estimated[9] from the line width of the C-1 signal. It may be noted, of course, that other values (e.g., 180° - ϕ, or 180° - ψ) are, hypothetically, consistent with these coupling constants.

Nonselective Spin–Lattice Relaxation Rates (R_1^{ns}). Although a rigorous and detailed analysis of molecular structure based on the relaxation behavior of a multispin system requires usage of the full density matrix formalism, valuable structural information may be acquired by an appropriate approximation. To a reasonable degree, the internuclear distances of interest in this study should be afforded by nonselective proton spin–lattice relaxation rates when they are governed primarily by ^1H–^1H dipolar interactions. That is, the latter, which are expected to be pairwise additive, decrease approximately with the sixth power of the internuclear distances. Nevertheless, other factors require attention: (a) the influence of mechanisms competing with interproton dipolar interactions, which should be minimal, (b) dipolar cross-relaxation effects, and (c) cross-correlation effects and motional anisotropy (if present).

In the present study, intermolecular dipolar contributions were kept to a minimum by restricting the relaxation measurements to a degassed, dilute solution. Other competing relaxation mechanisms were found to be absent, as shown by the ratios of the nonselective to monoselective relaxation rates for each proton (see below). Although problems associated with nonexponential decay and cross-correlation effects are often avoided by confining measurements to initial relaxation rates,[12,30] the latter procedure may be inadequate for strongly coupled nuclei. Consequently, the possible importance of these effects was assessed from the relaxation rates of individual lines in multiplets, which differ significantly in the presence of such effects. Notable differences were observed only for the two strongly coupled protons H-1 and H-2: 1.22, 0.96 s^{-1} for the H-1 doublet and 0.53, 0.41, 0.50, 0.42 s^{-1} for the H-2 quartet (ca. 20% variation).

Motional anisotropy was not a factor in the present study, since ^{13}C T_1 measurements indicated that **1** reorients isotropically as a whole. It is apparent from Table II that the ^{13}C T_1 values for ring carbons, each of which bears a single proton, are essentially the same. This is true as well for the methylene C-6 of the rigid anhydro ring, allowing for the contribution of two protons to its relaxation, whereas the methylene C-6 of the β-D-glucopyranosyl ring is characterized by a higher T_1 value, indicating an additional degree of freedom, i.e., rotation about the C-5–C-6 bond. Summarized in Table III are the R_1^{ns} values for **1** at 400 MHz, together with their ratios relative to the corresponding values of the resolved resonances at 200 MHz. These ratios are essentially constant, with an average value of 1.06 s, in agreement with a previous finding[31] that relaxation rates may be comparable even when obtained at different frequencies.

Although the nonselective relaxation rates of **1** may be interpreted in terms of conformation and the contributions of neighboring protons to the relaxation process, interesting information also is obtainable about the spatial arrangement of the protons involved in relaxation. According to the formalism[32] of the inverse sixth-root dependence of the dipole–dipole mechanism of spin–lattice relaxation, the ratios of interproton distances may be calculated by the approximate expression:

$$\frac{R_1(i-j)}{R_1(k-j)} = \left(\frac{r_{kj}}{r_{ij}}\right)^6 \quad (1)$$

where i and k are the donor nuclei and j is the receptor nucleus. Equation 1 presupposes a preponderance of the dipole–dipole mechanism, and also that the molecule is tumbling isotropically, conditions that are met in the present study, as noted previously.

The ratios in Table III were converted into interproton distances (r_{ij}) by taking the distance between the geminal protons of the anhydro ring $r_{H\text{-}6'b,H\text{-}6'b}$, as equal to that obtained from X-ray diffraction experiments,[18a,b] vis., 1.74 Å, and are listed in Table IV. These values differ appreciably from those obtained from crystallographic data for β-cellobiose and its octaacetate,[17a,b] and 1,6-anhydro-β-D-glucopyranose and its triacetate.[18a,b] Perhaps the main reason for this discrepancy is the simplified form of eq 1, which is concerned with an isolated three-spin system, with pairwise additivity in relaxation rates, whereas **1** is a more complex molecule wherein many interconnecting relaxation pathways[33] exist, and the concept of pairwise additivity may break down.

For more than qualitative information on molecular stereochemistry, it is necessary to utilize reliable separation techniques. Two such techniques are considered in the sections to follow.

Monoselective Spin–Lattice Relaxation Rates (R_1^s) and NOE Data. One separation technique involves a combination of monoselective relaxation rate measurements and NOE experiments. The theory[15,30,34] associated with these experiments states that for a nucleus, i, in a molecular environment of other nuclei, j, the nonselective spin–lattice relaxation rate, R_1^{ns} is described by

$$R_{1,i}^{ns} = \sum_{i\neq j}\rho_{ij} + \sum_{i\neq j}\sigma_{ij} + \rho^*_{ij} \quad (2)$$

The first term accounts for all pairwise direct dipolar contributions of spins j to spin i, whereas the second sum expresses the dipolar cross-relaxation between spins j and i, associated with the cross-relaxation transition probabilities in a coupled spin system that distort the recovery curve from its exponential form. All other relaxation contributions to the total relaxation rate of spin i, other than dipole–dipole interactions, are contained in the third term. To the extent that intramolecular dipole–dipole relaxation is the dominant relaxation mechanism, i.e., $\rho^*_{ij} << \sum_{i\neq j}\rho_{ij}$, the third term in eq 2 is omitted. It has been shown[15] that the first term of eq 2 can be equated with the monoselective relaxation rate provided that this quantity is measured in the initial rate approximation, i.e.,

$$R_{1,i}^{s} = \sum_{i\neq j}\rho_{ij} \quad (3)$$

Therefore eq 2, omitting the third term, becomes

$$R_{1,i}^{ns} = R_{1,i}^{s} + \sum_{i\neq j}\sigma_{ij} \quad (4)$$

In the extreme narrowing range, and for isotropic motion, the cross-relaxation parameter is given as

$$\sigma_{ij} = \rho_{ij/2} = 0.5\frac{\gamma_i^2\cdot\gamma_j^2\hbar^2}{r_{ij}^6}\tau_c(ij) \quad (5)$$

where r_{ij} is the distance between nuclei i and j and $\tau_c(ij)$ is the rotational correlation time of the vector $\mathbf{r}_{ij}$.

Since the NOE $f_i(j)$ of a spin i before and after irradiation of spin j is given[30] by

$$f_i(j) = \frac{\sigma_{ij}}{\sum_{i\neq j}\rho_{ij}} = \frac{\sigma_{ij}}{R_{1,i}^{s}} \quad (6)$$

(30) Noggle, J. H.; Shirmer, R. E. "*The Nuclear Overhauser Effect*"; Academic Press: New York, 1971.
(31) Bock, K.; Hall, L. D.; Pederson, C. *Can. J. Chem.* **1980**, *58*, 1916.
(32) Solomon, I. *Phys. Rev.* **1955**, *99*, 559.
(33) Contributions from acetyl protons are by no means negligible, particularly for the anhydro ring, where the acetyl protons have a high probability of being in a near-eclipsed arrangement relative to the ring protons.[18a]
(34) Campbell, I. D.; Dobson, C. D.; Ratcliffe, R. G.; Williams, R. J. P. *J. Magn. Reson.* **1978**, *29*, 397.

Table III. Spin-Lattice Relaxation Rates (in s^{-1}) of 2,3,4,6,2',3'-Hexa-*O*-acetyl-4-*O*-β-D-glucopyranosyl-1,6-anhydro-β-D-glucopyranose (1)[a] and Its Partially Deuterated Analogue (2)[a]

experiment	H-1	H-2	H-3	H-4	H-5	H-6a[b]	H-6a'[b]	H-1'	H-2'	H-3'	H-4'	H-5'	H-6'b	H-6'b'
						1								
nonselective														
400 MHz	1.05	0.48	0.53	0.51	0.99	1.56	1.56	0.36	0.44	0.54	0.88	0.72	1.49	1.49
200 MHz[c]			0.55		1.11	1.63		0.38	0.47	0.52	0.96	0.74		1.66
200/400 (MHz)			1.04		1.12	1.04		1.05	1.07	0.96	1.09	1.03		1.12
						2[d]								
nonselective	0.83				0.50			0.24			0.77	0.74	1.64	1.64
monoselective	0.55				0.33			0.16			0.51	0.50	1.10	1.11
R_i^{ns}/R_i^{s}[e]	1.51				1.51			1.50			1.51	1.51	1.49	1.48
bisselective														
R_1 (1,5)	0.62				0.40									
R_1 (1,4')	0.64										0.60			
R_1 (1,5')	0.56											0.51		
R_1 (4',5')											0.58	0.57		
R_1 (4',6'b')											0.60			1.15
R_1 (5',6'b)												0.62	1.19	
R_1 (5',6'b')												0.535		1.12

[a] Degassed 0.05 M solutions of 1 and 2 in acetone-d_6. [b] Notations a and b refer to the geminal protons of the glucopyranosyl and 1,6-anhydroglucopyranose residues, respectively. [c] Signals for H-1, -2, -4, -6a', and -6'b were unresolved. [d] Signals for H-2, -3, -4, -6a, -a', -2', and -3' were eliminated (≥90%) through deuteration. [e] The estimated statistical error in the various relaxation rates was better than ±5%, which yields a ±6% error in the relaxation rate ratio. The reproducibility in the various relaxation measurements was better than ±5%.

Table IV. ^{1}H Nuclear Overhauser Enhancement of 2,3,4,6,2',3'-Hexa-*O*-acetyl-d_{18}-4-*O*-β-D-glucopyranosyl-1,6-anhydro-β-D-glucopyranose-d_7 (2)

proton irradiated	proton observed[a]					
	H-1	H-5	H-4'	H-5'	H-6'b	H-6'b'
H-1		0.229 (±0.006)	0.131 (±0.006)	0.021 (±0.009)		
H-5	0.142 (±0.004)					
H-4'	0.128 (±0.006)			0.108 (±0.003)	−0.067 (±0.003)	0.100 (±0.004)
H-5'	0.013 (±0.008)		0.110 (±0.005)		0.104 (±0.005)	
H-6'b				0.204 (±0.006)		0.355 (±0.004)
H-6'b'			0.117 (±0.003)	0.052 (±0.008)	0.323 (±0.005)	

[a] Values in parentheses are standard deviations.

then rewriting eq 3 and 4 we obtain the sum of all possible NOEs on resonance i due to dipolar interactions with other protons:

$$R_{1,i}^{ns}/R_{1,i}^{s} = 1 + \sum_{i \neq j} f_i(j) = 1 + n_i(j) \quad (7)$$

As the maximum NOE obtained for dipolar interactions among similar spins is 50%, $n_i(j) = 0.5$ when the dipolar mechanism is preponderant, and the ratio of the nonselective to monoselective relaxation rates becomes 1.5. This is a useful criterion for examining the extent of dipolar interactions in a multispin system of protons.

Interatomic distances may be calculated after substitution of eq 6 into eq 5, i.e.,

$$r_{ij}^6 = \frac{0.5\gamma_i^2\gamma_j^2\hbar^2}{R_{1,i}^{s} f_i(j)}\tau_c(ij) \quad (8)$$

To reduce experimental time, as well as complexity,[35] without sacrifice of stereochemical information, compound 2, a partially deuterated analogue of 1, was used in these analyses. Values of $R_{1,i}^{s}$ obtained are given in Table III. It is worth noting that the ratios of the nonselective rates to monoselective rates for each proton, also contained in this table, are very close to the theoretical value of 1.5, which reaffirms the preponderance of dipole–dipole interactions in the relaxation of these protons. By use of eq 8, the $R_{1,i}$ values of Table III, and those of NOE in Table IV, average interproton distances were calculated (Table V). A value of $\tau_c(ij)$ equal to $46.6 \pm 0.15 \times 10^{-12}$ s was obtained from the average of the ^{13}C T_1 values of the ring carbons of 1 (Table II), and the well-known expression[30] describing isotropic overall molecular reorientation in the extreme narrowing region. Two r_{ij} determinations, within the error limits cited, were obtained for each pair of spins, where the appropriate NOEs were measured experimentally (Table IV). Clearly, the internuclear distances between protons of the individual rings of 2 are in good agreement with those obtained by X-ray diffraction for β-cellobiose and 1,6-anhydro-β-D-glucopyranose, and their *O*-acetyl derivatives. X-ray diffraction studies[18a,b] have shown that the 1,6-anhydro-β-glucopyranose chair is flattened upon acetylation, so that the distance of C-3 from the mean plane defined by C-1, C-4, and C-5 is decreased by 0.05 Å whereas, otherwise, the geometry of the anhydro ring remains unchanged. Similarly subtle modifications in the geometry of β-cellobiose upon acetylation also have been observed for the solid state.[17a,b] It would not be anticipated that geometric alterations of this order in solution are detected by monoselective and NOE experiments. Nevertheless, such features as the $^1C_4$ conformation adopted by the anhydro moiety are clearly reflected in the interproton distances obtained from NMR.

As noted previously, the most probable conformation of the glucosidic bond is reflected in the H-1–H-4' and H-1–H-5' distances determined from the NMR data. These values may be compared with the computer-generated distances as a function

(35) For instance, deuteration at C-2 eliminated the dipolar contribution of H-2 to the relaxation of H-1, thereby simplifying the examination of the effect of H-5' upon H-1.

Table V. Interproton Distances (Å) for 2,3,4,6,2',3'-Hexa-*O*-acetyl-4-*O*-β-glucopyranosyl-1,6-anhydro-β-D-glucopyranose (**1**)

	protons (*i*,*j*)													
	1,2	2,3	3,4	4,5	1,5	1,4'	1,5'	4',5'	3',4'	4',6'b'	5',6'b	5',6'b'	2',3'	1',2'	6'b,6'b'
r_{ij} from X-ray diffraction data	2.98[a]	2.91[a]	2.90[a]	2.97[a]	2.51[a]	2.21[a]	4.06[a]	2.47[b]	2.49[b]	2.33[b]	2.19[b]	2.63[b]	2.41[b]	2.53[b]	1.74[b]
	3.04[c]	2.85[c]	2.95[c]	3.08[c]	2.30[c]	2.57[c]	3.98[c]	2.29[d]	2.35[d]	2.44[d]	2.49[d]	2.73[d]	2.80[d]	2.29[d]	1.72[d]
r_{ij} from R_1^{ns} data	2.22	2.49	2.51	2.25	2.23	2.01	2.08	2.14	2.25	1.90	1.96	1.96	2.32	2.58	
r_{ij} from R_1^{s} and NOE data[e]					2.35	2.42	3.29	2.50		2.22	2.21	2.78			1.82
					(±0.05)	(±0.06)	(±0.20)	(±0.02)		(±0.03)	(±0.008)	(±0.09)			(±0.05)
					2.37	2.39	3.51	2.49		2.46	2.25				1.80
					(±0.08)	(±0.04)	(±0.15)	(±0.03)		(±0.05)	(±0.05)				(±0.07)
r_{ij} from R_1^{s} and R_1^{bs} data[e]					2.40	2.30	3.31	2.39		2.80	2.20	2.69			
					(±0.12)	(±0.08)	(±0.15)	(±0.06)		(±0.07)	(±0.06)	(±0.10)			
								2.63[f]			2.30[f]	3.31[f]			
								(±0.07)			(±0.05)	(±0.20)			

[a] Interproton distances of β-cellobiose from ref 17b; error ±0.01 Å. [b] Interproton distances of 1,6-anhydro-β-D-glucopyranose from ref 18b; error ±0.01 Å. [c] Interproton distances of β-cellobiose octaacetate from ref 17a; error ±0.05 Å. [d] Interproton distances of 2,3,4-*O*-triacetyl-1,6-anhydro-β-D-glucopyranose from ref 18a; error ±0.05 Å. [e] Error calculations based on the errors of the measured quantities in eq 8 and 9. [f] Interproton distances calculated from the relaxation parameters of the methylene protons.

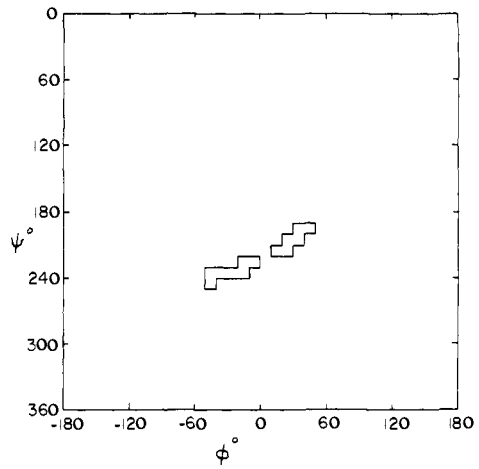

Figure 4. Allowed conformations (enclosed by solid line) of the glucosidic bond of **1**, calculated as a function of the H-1–H-4' and H-1–H-5' interatomic distances (see text).

of torsional angles ϕ and ψ. However, within the limit of experimental error (ca. ±0.2 Å), computer simulation shows that several sets of ϕ and ψ angles conform with the NMR values. These conformations are depicted in Figure 4 in the form of a "conformational map", wherein the region of the allowed conformations is enclosed by a solid line, corresponding to a range for ϕ of from −50 to +50°, and for ψ from 190–250° (or 10–70°). Included among the allowed conformations are those derived from coupling constants. Nevertheless, the relaxation and NOE data suffer from the same limitations as coupling constants. For instance, one cannot distinguish between a freely rotating and fixed conformation, because the experiments involved reflect a thermodynamically averaged geometry, rather than a difference between various energy minima attained by certain allowed conformations of the glucosidic bond. Another difficulty lies in distinguishing between angles of ϕ and 180° − ϕ, or ψ and 180° − ψ.

Crystallographic interproton distances for H-1–H-4' and H-1–H-5' in β-cellobiose and its acetate derivative (Table V) are consistent with dihedral angles for ψ of −13.7 and +15.7°, respectively,[18a,b] whereas angle ϕ is 44.6° in both compounds. According to optical rotatory[7,36] and NMR studies,[10] these angles closely describe the orientation of the glucosidic bond of β-cellobiose and its octaacetate in solution. If this is true, then it may be concluded that the conformation of the glucosidic linkage of anhydride **1** differs appreciably from that of β-cellobiose octaacetate.

Monoselective (R^s) and Biselective (R_1^{bs}) Relaxation Rates. Another solution to the overall structural problem is possible when two nuclei are excited simultaneously and the biselective spin–lattice relaxation rate is measured. The relationship which holds between monoselective and biselective relaxation rates for two spins *i* and *j*, is

$$R_{1,i}^{bs} = R_{1,i}^{s} + \sigma_{ij} \text{ and/or } R_{1,j}^{bs} = R_{1,j}^{s} + \sigma_{ji} \qquad (9)$$

where $\sigma_{ij} = \sigma_{ji}$ the cross-relaxation term.

In this type of experiment, the cross-relaxation time involving only those two spins can be isolated and the interproton distances can be calculated from eq 9 and 5. Various calculated distances for **2** obtained from mono- and biselective relaxation rates (Table III) of the pertinent pairs of protons are given in Table IV; since σ_{ij} equals σ_{ji}, within experimental error, one value is listed for each interproton distance. It is apparent that these parameters are in general agreement with those obtained from the monoselective relaxation rate and NOE data. However, some discrepancies are observed for distances calculated for the geminal protons of the anhydro ring. This is due mainly to inherent experimental limitations in the biselective experiments for these protons. If the

(36) Rees, D. A.; Thom, D., *J. Chem. Soc., Perkin Trans. 2* **1977**, 191.

pulse duration is long enough, and comparable to the relaxation time of a multiplet, then relaxation may occur during excitation, which results in an incomplete inversion of the multiplet by the initial selective 180° pulse, and/or in a distortion of the recovery curve obtained by using the 90° monitoring pulse. It is reasonable to believe that if the spin–lattice relaxation times are more than ~ 20–50 times longer than pulse durations, relaxation during the pulses may safely be ignored. However, the relaxation times of the geminal protons of **2** are only eight times longer than the pulse duration used (100 ms), thereby introducing a systematic error into the calculation of their interproton distances.

Conclusion

Various sets of experiments have been used to determine the conformation of the glucosidic bond of **1**. Different selective relaxation experiments gave comparable results, which are in agreement with coupling constant data, whereas nonselective relaxation rates alone failed to give accurate quantitative results because of the limitations discussed, as has been encountered in other relaxation studies of multispin systems. For simpler systems, however (e.g., see ref 11), the nonselective relaxation measurements may be closely consistent with X-ray data.

Acknowledgment. This work was generously supported by the Natural Sciences and Engineering Research Council of Canada, and McGill University. We are especially grateful to George Fainos for writing the computer program used in generating the data of Figure 4. The 400-MHz spectra were recorded at Laboratoire Regional de RMN à Haut Champ, Université de Montréal.

Registry No. 1, 38631-27-5.

300-MHz ^{1}H NMR Study of Parabactin and Its Gallium(III) Chelate

Raymond J. Bergeron* and Steven J. Kline†

Contribution from the Department of Medicinal Chemistry, J. Hillis Miller Health Center, University of Florida, Gainesville, Florida 32610. *Received April 8, 1983*

Abstract: The solution structure of parabactin and its gallium(III) complex is evaluated with 300-MHz ^{1}H NMR. The ligand is shown to exist in three separate conformers while the chelate appears to form the Λ cis chelate exclusively. Furthermore, the chelate is shown to exist in a 3:1 ratio of two diastereomeric forms that differ only in the disposition of the spermidine backbone.

Siderophores are relatively low molecular weight, virtually ferric ion specific ligands. These chelators are produced by microorganisms for the purpose of sequestering exogenous ferric ion and facilitating the transport of this biologically essential metal across the cell membrane.[1,2] The two major classes of siderophores, hydroxamates and catecholamides,[3-7] both from very stable octahedral, high-spin iron(III) complexes with formation constants in excess of 10^{30}. Enterobactin, for example, a cyclic triester of (2,3-dihydroxybenzoyl)serine, is the strongest ferric ion chelating agent known.[8] At pH 7.4, the enterobactin–iron(III) formation constant is 10^{52}. However, much less is known about the spermidine catecholamide siderophore, parabactin (Figure 1), first isolated from an iron-depressed culture of *Paracoccus denitrificans* by Tait in 1975.[9] Since the original isolation of parabactin, most of the studies on this ligand have been focused on the synthesis of this siderophore and its analogues.[10] Little attention has been given to the solution structure of the ligand or its metal complex.

The utilization of a ferric chelate by a microorganism begins with its recognition and transport by membrane receptors. The transport of siderophore metal chelates across microbial cell membranes has been shown in several instances to be stereospecific.[11-13] The recognition of siderophore iron chelates by the microorganism's outer membrane receptors may depend on the configuration of the chelate about the metal center itself, the conformation of various groups in the ligand, or both. As an initial step in a program to evaluate parabactin–receptor interactions, the solution conformation and stereochemistry of parabactin and its gallium chelate was studied.

Experimental Section

General. All reagents, with the exception of L-(*tert*-butoxycarbonyl)threonine (Sigma Chemical) and gallium(III) nitrate–$9H_2O$ (Alfa) were purchased from Aldrich Chemical Co. and were used without further purification. Na_2SO_4 was used as a drying agent. Melting points were taken on a Fisher–Johns apparatus and are uncorrected. Preparative thin-layer chromatography was done on 20 × 20 cm silica gel plates obtained from Analtech. Sephadex LH-20 was purchased from Pharmacia Fine Chemicals. Optical rotations were measured with a Perkin-Elmer Model 141 polarimeter. Elemental analyses were performed by Galbraith Laboratories, Knoxville, TN, or Atlantic Microlab Inc., Atlanta, GA. Proton NMR spectra were obtained on a Nicolet Instrument Corp. NT-300 spectrometer and NIC-1180 E data system. Probe temperature was determined with test samples of ethylene glycol. Computer simulation and curve analysis/deconvolution programs used were included in the NMCFT software package provided by Nicolet Technology Corp. Resolution enhancement, when necessary, was performed by apodization of the FID by a double-exponential multiplication followed by zero filling. Samples for the determination of temperature of coalescence were prepared by dissolving 5–10 mg of the compound in 500 μL of Me_2SO-d_6. Coalescence temperatures, ±1 °C, were then deter-

† Current address: Abbott Laboratories, Abbott Park, IL 60064.

(1) Neilands, J. B. In "Microbial Iron Metabolism"; Neilands, J. B., Ed.; Academic Press: New York, 1974; pp 3–34.
(2) Emery, T. In "Metal Ions in Biological Systems"; Sigel, H., Ed.; Marcel Dekker: New York, 1978; Vol. 7, pp 77–125.
(3) Neilands, J. B. *Ann. Rev. Biochem.* **1981**, *50*, 715–731.
(4) Raymond, K. N.; Carrano, C. J. *Acc. Chem. Res.* **1979**, 183–190.
(5) Neilands, J. B. *Ann. Rev. Nutr.* **1981**, *1*, 27–46.
(6) Raymond, K. N. *Adv. Chem. Ser.* **1977**, *162*, 33–54.
(7) Neilands, J. B.; Peterson, T.; Leong, S. A. In "Inorganic Chemistry in Biology and Medicine"; Martell, A. E., Ed.; American Chemical Society: Washington, DC, 1980; pp 263–278.
(8) Harris, W. R.; Carrano, C. J.; Raymond, K. N. *J. Am. Chem. Soc.* **1979**, 101, 2213–2214.
(9) Tait, G. H. *Biochem. J.* **1975**, *146*, 191–204.
(10) Bergeron, R. J.; Kline, S. J. *J. Am. Chem. Soc.* **1982**, *104*, 4489–4492.
(11) Winkelmann, G. *FEBS Lett.* **1979**, *97*, 43–46.
(12) Neilands, J. B.; Erickson, T. J.; and Rastettler, W. H. *J. Biol. Chem.* **1981**, *265*, 3831–3832.
(13) Winkelmann, G.; Braun, V. *FEMS Microbiol. Lett.* **1981**, *11*, 237–241.

0002-7863/84/1506-3089$01.50/0